remote sensing

MDPI

Article

The Synchrosqueezed Method and Its Theory-Analysis-Based Novel Short-Time Fractional Fourier Transform for Chirp Signals

Zhen Li [1], Zhaoqi Gao [1], Liang Chen [2], Jinghuai Gao [1,*] and Zongben Xu [3]

[1] The National Engineering Research Center for Offshore Oil and Gas Exploration, School of Information and Communications Engineering, Xi'an Jiaotong University, Xi'an 710049, China; zhen_li@xjtu.edu.cn (Z.L.); zq_gao@xjtu.edu.cn (Z.G.)
[2] Department of Mathematics, Jiujiang University, Jiujiang 332005, China; chenliang3@mail2.sysu.edu.cn
[3] School of Mathematics and Statistics, Xi'an Jiaotong University, Xi'an 710049, China; zbxu@mail.xjtu.edu.cn
* Correspondence: jhgao@mail.xjtu.edu.cn

Abstract: Time–frequency analysis is an important tool used for the processing and interpretation of non-stationary signals, such as seismic data and remote sensing data. In this paper, based on the novel short-time fractional Fourier transform (STFRFT), a new modified STFRFT is first proposed which can also generalize the properties of the modified short-time Fourier transform (STFT). Then, in the modified STFRFT domain, we derive the instantaneous frequency estimator for the chirp signal and present a new type of synchrosqueezing STFRFT (FRSST). The proposed FRSST presents many results similar to those of the synchrosqueezing STFT (FSST), and it extends the harmonic signal to a chirp signal that offers attractive new features. Furthermore, we provide a detailed analysis of the signal reconstruction, theories, and some properties of the proposed FRSST. Several experiments are conducted, and all of the results illustrate that the proposed FRSST is more effective than the FSST. Finally, based on the linear amplitude modulation and frequency modulation signal, we present a derivation for analyzing the limitations of the FRSST.

Keywords: novel short-time fractional Fourier transform; synchrosqueezing STFT; synchrosqueezing STFRFT; theory analysis

Citation: Li, Z.; Gao, Z.; Chen, L.; Gao, J.; Xu, Z. The Synchrosqueezed Method and Its Theory-Analysis-Based Novel Short-Time Fractional Fourier Transform for Chirp Signals. *Remote Sens.* **2024**, *16*, 1173. https://doi.org/10.3390/rs16071173

Academic Editors: Xiuping Jia, Ran Tao, Junhui Hou and Shaohui Mei

Received: 7 December 2023
Revised: 22 March 2024
Accepted: 24 March 2024
Published: 27 March 2024

1. Introduction

The Fourier transform (FT) is a fundamental technique used to process and interpret signals [1,2]. It can detect the frequency contents within the signal, and it has been widely applied in speech processing, quantum physics, and remote sensing images. As a generalization of the FT, the fractional FT (FRFT) was designed in the mathematics literature [3,4]. Both the FT and FRFT are global transformations that cannot describe the time location of a frequency or fractional frequency. However, as we know, most actual signals are time-varying frequencies. Thus, it is often necessary to localize the frequency characteristics as they change over time. For this goal, the time–frequency analysis (TFA) method is an effective and important tool that obtains the characterization of time-varying frequencies. Based on the FT, many classical TFA methods have been proposed, such as the short-time FT (STFT), wavelet transform (WT), S transform (ST), Wigner–Ville distribution (WVD), and Cohen class distribution [5–13]. As developments of the FRFT, short-time FRFT (STFRFT), fractional wavelet transform (FRWT), and fractional ST were also designed [14–19]. All of these TFA tools can analyze the location of the signal frequency response. Unfortunately, due to Heisenberg's uncertainty principle, traditional methods always provide diffused time–frequency representations (TFRs).

For FT-based TFR, to improve the quality and readability, many methods have been proposed. Among the post-processing tools, the synchrosqueezing transform (SST) is one of the most representative techniques [20,21]. In fact, the SST can be regarded as a special situation of the reassigned method [21,22]. The SST retains superiority in concentrated energy and further allows for signal reconstruction [23]. The SST has, thus, been widely extended and studied. On the one hand, the original SST is based on the CWT, and the innovation was introduced into other classical transforms, such as the STFT, ST, and GST [24–26]. On the other hand, the translation direction of TF coefficients changes from the frequency to the time, such the time-reassigned SST and the transient-extracting transform [27–30]. Moreover, a higher-order expansion of the amplitude and the phase are introduced into the time or frequency domain, which improves the concentration and adaptability of the SST-based method, such as the second-order SST, second SET [31–35], and high-order SST or SET [36,37]. A higher order can provide a more highly concentrated TFR but requires more complex computation. In fact, the SST also inspires some other ideas, such as the multisynchrosqueezing (MSST) and synchroextracting transforms (SET) [38,39], which have also drawn significant attention [40–44]. In conclusion, a perfect system of theory and method for the FT-based SST already exists.

For FRFT-based approaches, it is just the beginning. Considering the resolution and concentration, FRFT-based methods are combined with the idea of the SST. The synchrosqueezed fractional wavelet transform (FRWSST) and synchrosqueezing-based short-time fractional Fourier transform methods have been proposed [45–47]. In the FRWSST, theory analysis was built and superiority was shown. In this study, we focus on the paper concerning synchrosqueezing-based short-time fractional Fourier transform [47]. The author provided a corresponding definition, some derivations, and simple calculations, but no systemic mathematical analysis of the approximation theory and properties is available. In our work, the main aim is to bridge this gap.

In fact, there are many different definitions of the STFRFT [14–16], but most of these definitions cannot generalize the classical result of the STFT that is interpreted as a bank of filters [48]. To deal with this issue, a novel STFRFT was proposed [48]. In this study, to achieve this goal, we design a modified STFRFT based on the novel STFRFT, and then propose a new fractional synchrosqueezing transform. For the theoretical analysis of errors of instantaneous frequency (IF) estimation and mode reconstruction, we extend the harmonic wave-like signal class to the chirp-like ones. Then, we present a new approximation result that differs slightly from the Fourier-based SST (FSST) [24], and also study some of the properties of the proposed method. Furthermore, we present an analysis of the inapplicability of the approach for linear amplitude modulation signals.

This paper is organized as follows. In Section 2, we briefly review the FRFT and STFRFT. In Section 3, a new FRSST and the corresponding theoretical analysis of the approximation theorem and some of its properties are presented. In Section 4, composite examples are used to demonstrate the performance of the proposed FRSST. Finally, a brief discussion and conclusion are presented in Sections 5 and 6.

2. Preliminaries

2.1. Fractional Fourier Transform

The fractional Fourier transform (FRFT) is one of the unitary integral transforms. For one given signal $f(t) \in L^2(\mathbb{R})$, the definition of the FRFT is [4]

$$F_\alpha(u) = \mathcal{F}^\alpha\{f(t)\}(u) = \int_{\mathbb{R}} f(t)\mathcal{K}_\alpha(t,u)dt \tag{1}$$

The kernel $\mathcal{K}_\alpha(t,u)$ is

$$\mathcal{K}_\alpha(t,u)\begin{cases} B_\alpha e^{j\frac{u^2+t^2}{2}\cot\alpha - jut\csc\alpha}, & \alpha \neq m\pi \\ \delta(t-u), & \alpha = 2m\pi \\ \delta(t+u), & \alpha = (2m-1)\pi \end{cases} \tag{2}$$

where $B_\alpha = \sqrt{(1-j\cot\alpha)/2\pi}$ and $m \in \mathbb{Z}$, $\delta(\cdot)$ is the Dirac Delta function, and t and u are the time and fractional frequency, respectively. Like the Fourier transform (FT) spectrum, the FRFT can only provide fractional frequencies within the signal, but it cannot localize frequency characteristics that change with time. Like the short-time FT (STFT), as is well known, the simplest solution is the short-time FRFT (STFRFT) that gives the information of the signal in time and frequency domains [14].

2.2. Short-Time FRFT

Indeed, there are many different STFRFTs proposed in the literature [49–51], but none of those definitions can generalize the properties of the STFT. In this situation, Shi et al. proposed a novel STFRFT [48]:

$$STFRFT_f^{\alpha}(t,u) = \int_{\mathbb{R}} f(\tau) g_{\alpha,t,u}^{*}(\tau) d\tau \tag{3}$$

where

$$g_{\alpha,t,u}(\tau) \triangleq g(\tau - t) e^{-j\frac{\tau^2 - t^2}{2}\cot\alpha + j\tau u \csc\alpha} \tag{4}$$

Like the STFT, due to the fixed window, the STFRFT will obtain a TFR with diffused energies. In fact, a synchrosqueezing-based STFRFT has been proposed [47]. However, to our knowledge, no thorough theory is available. In this paper, to bridge that gap, we propose a new synchrosqueezing transform based on the modified novel STFRFT defined by (5).

3. FRSST-Based Novel STFRFT

3.1. Modified Novel STFRFT

Inspired by the modified STFT, we introduce a phase shift $e^{jut\csc\alpha}$ into the novel STFRFT (3), and then define the modified STFRFT as

$$STFRFT_f^{\alpha}(t,u) = \int_{\mathbb{R}} f(\tau) g(\tau - t) e^{j\frac{\tau^2 - t^2}{2}\cot\alpha - ju(\tau - t)\csc\alpha} d\tau \tag{5}$$

In consideration of the novel STFRFT [48], the modified STFRFT (5) can preserve the properties of the modified STFT well, and has the following equivalent form:

$$STFRFT_f^{\alpha}(t,u) = \int_{\mathbb{R}} F_{\alpha}(u') G^{*}\big((u' - u)\csc\alpha\big) \mathcal{K}_{\alpha}^{*}(t,u') du' \tag{6}$$

where $G^{*}(\cdot)$ means the FT of $g(t)$.

3.2. Definition of the New FRSST

To motivate the new synchrosqueezing short-time FRFT (FRSST), it considers a chirp signal $f(t) = Ae^{j\phi(t)}$, where $\phi(t) = a + \omega_0 t + \frac{1}{2}ct^2$, and a Gaussian window function $g(t) = e^{-\sigma t^2}$. Obviously,

$$f(\tau + t) = f(t) e^{i[\phi'(t)\tau + \frac{1}{2}\phi''(t)\tau^2]}$$

According to (6) and letting $\alpha = -\text{arccot}(c)$, we can obtain the FRFT of $f(t)$ as

$$F_{\alpha}(u) = B_{\alpha} |\sin\alpha| A e^{j\frac{\omega_0^2}{4}\sin 2\alpha} \delta(u - \omega_0 \sin\alpha) \tag{7}$$

Substituting (7) into (6),

$$STFRFT_f^{\alpha}(t,u) = \frac{A}{2\pi} \hat{G}(\omega_0 - u\csc\alpha) e^{j\phi(t)}$$

Then, we calculate the derivative of the STFRFT as

$$\begin{aligned} \partial_t STFRFT_f^{\alpha}(t,u) &= j\phi'(t) \tfrac{A}{2\pi} \hat{G}(\omega_0 - u\csc\alpha) e^{j\phi(t)} \\ &= j\phi'(t) STFRFT_f^{\alpha}(t,u) \end{aligned} \tag{8}$$

It holds that

$$\frac{\partial_t STFRFT_f^{\alpha}(t,u)}{jSTFRFT_f^{\alpha}(t,u)} = \phi'(t) = \omega_0 + ct \tag{9}$$

Alongside the FSST, we can define the frequency estimation operator $\omega_f^{\alpha}(t,\omega)$ in the modified STFRFT domain as

$$\widetilde{\omega}_f^{\alpha}(t,u) = \Re\left\{\frac{\partial_t STFT_f^{\alpha}(t,u)}{jSTFT_f^{\alpha}(t,u)}\right\} \tag{10}$$

Therefore, the new time–frequency-representative FRSST can be defined as

$$FRSST_f^{\alpha}(t,\omega) = \int_{\Xi_f^{\alpha}} STFRFT_f^{\alpha}(t,u)\delta\Big(\omega - \widetilde{\omega}_f^{\alpha}(t,u)\Big)du \tag{11}$$

where $\Xi_f^{\alpha} \triangleq \left\{u \in \mathbb{R}^+ \middle| STFRFT_f^{\alpha}(t,u) \neq 0\right\}$. If the $\alpha = \pi/2$, the proposed FRSST becomes the conventional FSST. It is worth noting that the proposed FRSST preserves some properties of the conventional FSST, which will be analyzed in detail. Similar to the FSST [24,31], the FRSST only reassigns the coefficients and does not lose any information. The FRSST, thus, allows for the reconstruction of the signal, which can be proven by the following expression:

$$\begin{aligned} \int_{\mathbb{R}} FRSST(t,\omega)d\omega &= \int\int_{\mathbb{R}\times\mathbb{R}^+} STFRFT_f^{\alpha}(t,u)\delta\Big(\omega - \widetilde{\omega}_f^{\alpha}(t,u)\Big)dud\omega \\ &= \int_{\mathbb{R}} STFRFT_f^{\alpha}(t,u)du \\ &= \int_{\mathbb{R}} F_{\alpha}(u')\mathcal{K}_{\alpha}^{*}(t,u')\int_{\mathbb{R}^+} G^{*}((u'-u)\csc\alpha)dudu' \\ &= \frac{2\pi}{\csc\alpha}g^{*}(0)\int_{\mathbb{R}} F_{\alpha}(u')\mathcal{K}_{\alpha}^{*}(t,u')du' \\ &= \frac{2\pi}{\csc\alpha}g^{*}(0)f(t) \end{aligned} \tag{12}$$

Equation (12) illustrates that the proposed FRSST can restore the original signal. The corresponding inverse FRSST is defined by

$$f(t) = \frac{\csc\alpha}{2\pi g^{*}(0)}\int_{\mathbb{R}} FRSST(t,\omega)d\omega \tag{13}$$

3.3. Theoretical Analysis of FRSSTT

In this section, we define a class of functions like the linear chirp that are well-separated and give an approximation result to show that the proposed new FRSST can successfully handle the defined class of signals. We start with the following definitions and propositions.

Definition 1. *Let $\varepsilon > 0$, $c > 0$ and $\Delta > 0$. The set $A_{\Delta,\varepsilon,c}$ of multicomponent signals $f(t)$ is the set of all multicomponent signals with the amplitude $A_n(t)$ and phase $\phi_n(t)$ satisfying the following conditions:*

$$\begin{aligned} &A_n(t) \in C^1(\mathbb{R}) \cap L^{\infty}(\mathbb{R}),\ \phi_n(t) \in C^2(\mathbb{R}), \\ &\sup_{t\in R}\phi'_n(t) < \infty,\ \phi'_n(t) > 0\ \forall t \in \mathbb{R}, \\ &|A'_n(t)| \leq \varepsilon,\ |\phi''_n(t) - c| \leq \varepsilon\ \forall t \in \mathbb{R}. \end{aligned}$$

Further, $f_n(t) = A_n(t)e^{j\phi_n(t)}$ are separated with the fractional resolution Δ, i.e., for all $n \in \{1,\ldots,N-1\}$ and all t,

$$\phi'_{n+1}(t) - \phi'_n(t) \geq 2\Delta$$

Definition 2. *Let function $h(t) \in C^{\infty}(\mathbb{R})$ and $\int h(t)dt = 1$, and set the threshold $\widetilde{\varepsilon}$ and the accuracy λ. The FRSST of $f(t) \in A_{\Delta,\varepsilon,c}$ with $\widetilde{\varepsilon}$ and λ can be defined by:*

$$FRSST_f^{\lambda,\widetilde{\varepsilon}}(t,\omega) = \frac{\csc\alpha}{2\pi g(0)}\int_{\Xi_f^{\alpha}} STFRFT_f^{\alpha}(t,u)\frac{1}{\lambda}h\left(\frac{\omega - \widetilde{\omega}_f^{\alpha}(t,u)}{\lambda}\right)du \tag{14}$$

where $\Xi_f^{\alpha} \triangleq \left\{u \in \mathbb{R}^+ \middle| STFRFT_f^{\alpha}(t,u) \neq 0\right\}$. When $\widetilde{\varepsilon}$ and λ approach zero, we obtain the usual formula as in (11).

Without the loss of generality, assuming $s \geq 0$ and according to Definition 1, for $\forall n \in \{1,\ldots,N\}$, the following can easily be obtained:

$$|A(t+s) - A(t)| = \int_0^s A'_n(t+\xi)d\xi \leq \varepsilon s \tag{15}$$

and

$$\left|\phi'_n(t+s) - \phi'_n(t) - cs\right| = \int_0^s (\phi''_n(t+\xi) - c)d\xi \leq \varepsilon s \tag{16}$$

Furthermore, for any $n \in \{1,\ldots,N\}$ and $t_0 \in \mathbb{R}$,

$$\phi_n(t) - \frac{c}{2}t^2 = \phi_n(t_0) - \frac{c}{2}t_0^2 + \left(\phi'_n(t_0) - ct_0\right)(t - t_0) + \int_0^{t-t_0}\left(\phi'_n(t_0+s) - \phi'_n(t_0) - cs\right)ds \tag{17}$$

Under these definitions and equivalences, we present the following two propositions:

Proposition 1. *For the multicomponent signals $f(t) = \sum_{n=1}^{N} f_n(t)$ and any $(t,u) \in \mathbb{R}^2$, it leads to*

$$\left|STFRFT_f^{\alpha}(t,u) - \sum_{n=1}^{N} f_n(t)G\left(u\csc\alpha - \left(\phi'_n(t) - ct\right)\right)\right| \leq \varepsilon\Gamma_1(t) \tag{18}$$

where $\Gamma_1(t) = NI_1 + \frac{1}{2}I_2\sum_{n=1}^{N} A_n(t)$, and $I_k = \int_{\mathbb{R}} |x|^k |g(x)|dx$.

Proof. See Appendix A. □

Proposition 2. *For the partial derivative $\partial_t STFRFT_f^{g}(t,u)$,*

$$\left|\partial_t STFRFT_f^{\alpha}(t,u) - j\sum_{n=1}^{N} f_n(t)\phi'_n(t)G\left(u\csc\alpha - \left(\phi'_n(t) - ct\right)\right)\right| \leq \varepsilon(\Gamma_2(t) + |u\csc\alpha + ct|\Gamma_1(t)) \tag{19}$$

where $\Gamma_2(t) = NI'_1 + \frac{1}{2}I'_2\sum_{n=1}^{N} A_n(t)$, and $I_k = \int_{\mathbb{R}} |x|^k |g'(x)|dx$.

Proof. See Appendix B. □

Proposition 1 and Proposition 2 extend the signal class to chirp-like ones and generalize the FT domain to FRFT. Based on these definitions and propositions, we present the following approximation theorem of the proposed new FRSST.

Theorem 1. *Consider $f(t) \in A_{\Delta,\varepsilon,c}$ and set $\widetilde{\varepsilon} = \varepsilon^{\frac{1}{3}}$. Let $g(t) \in S(\mathbb{R})$, the Schwartz class, satisfy $supp(\hat{g}) \subset [-\Delta,\Delta]$. Further, if ε is small enough, then*

(a) $\left|STFRFT_f^{\alpha}(t,u)\right| > \widetilde{\varepsilon}$ only when there exists $n \in \{1,\ldots,N\}$ such that $(t,u) \in Z_n := \{(t,u), s.t. |u\csc\alpha - (\phi'_n(t) - ct)| < \Delta\}$.

(b) For each $n \in \{1, \dots, N\}$ and all $(t, u) \in Z_n$ such that $\left|STFRFT_f^{\alpha}(t, u)\right| > \widetilde{\varepsilon}$,

$$\left|\widetilde{\omega}_f^{\alpha}(t, u) - \phi'_n(t)\right| \leqslant \widetilde{\varepsilon} \tag{20}$$

(c) Moreover, for all $n \in \{1, \dots, N\}$ and $\forall t \in \mathbb{R}$, there is a C such that

$$\left|\lim_{\lambda \to 0}\left(\frac{\csc\alpha}{2\pi g(0)}\int_{|\widetilde{\omega}_f(t,u)-\phi'_n(t)|\le\widetilde{\varepsilon}} FRSST_f^{\lambda,\widetilde{\varepsilon}}(t, \omega)d\omega\right) - f_n(t)\right| \leqslant C\widetilde{\varepsilon} \tag{21}$$

Proof. Different from the FSST, this theorem provides a strong approximation result for the chirp-like signal class in the FRFT domain. Furthermore, it only uses the first-order derivative of the STFRFT. Inspired by the FSST, the descriptions of the proof are shown in Appendix C. □

3.4. Basic Properties of the FRSST

Benefited by the novel STFRFT, the proposed FRSST also shares some properties with the FSST. Here, we list several of the most representative properties along with the corresponding proof.

(1) Linearity: For $f_1(t),\ f_2(t) \in A_{\Delta,\varepsilon,c}$ and two scalar constants $m_1,\ m_2$, let $f = m_1 f_1 + m_2 f_2$, and it holds

$$FRSST_f^{\alpha}(t, \omega) = m_1 FRSST_{f_1}^{\alpha}(t, \omega) + m_2 FRSST_{f_2}^{\alpha}(t, \omega) \tag{22}$$

Proof. Similar to the modified STFT, the proposed modified STFRFT is also linear, i.e.,

$$STFRFT_f^{\alpha}(t, u) = m_1 STFRFT_{f_1}^{\alpha}(t, u) + m_2 STFRFT_{f_2}^{\alpha}(t, u). \tag{23}$$

Following Theorem 1,

$$STFRFT_f^{\alpha}(t, u) = \begin{cases} m_1 STFRFT_{f_1}^{\alpha}(t, u), & u \in \left(\frac{(\phi'_1(t)-ct)-\Delta}{\csc\alpha}, \frac{(\phi'_1(t)-ct)+\Delta}{\csc\alpha}\right) \\ m_2 STFRFT_{f_2}^{\alpha}(t, u), & u \in \left(\frac{(\phi'_2(t)-ct)-\Delta}{\csc\alpha}, \frac{(\phi'_2(t)-ct)+\Delta}{\csc\alpha}\right) \\ \le \varepsilon^{\frac{1}{3}}, & \text{otherwise.} \end{cases} \tag{24}$$

Then, according to (10),

$$\widetilde{\omega}_f^{\alpha}(t, u) = \Re\left\{\frac{\partial_t STFT_f^{\alpha}(t, u)}{jSTFT_f^{\alpha}(t, u)}\right\} = \Re\left\{\frac{\partial_t\left(m_1 STFRFT_{f_1}^{\alpha}(t, u) + m_2 STFRFT_{f_2}^{\alpha}(t, u)\right)}{j\left(m_1 STFRFT_{f_1}^{\alpha}(t, u) + m_2 STFRFT_{f_2}^{\alpha}(t, u)\right)}\right\} \tag{25}$$

which, alongside (24), can obtain

$$\widetilde{\omega}_f^{\alpha}(t, u) = \begin{cases} \widetilde{\omega}_{f_1}^{\alpha}(t, u), u \in \left(\frac{(\phi'_1(t)-ct)-\Delta}{\csc\alpha}, \frac{(\phi'_1(t)-ct)+\Delta}{\csc\alpha}\right) \\ \widetilde{\omega}_{f_2}^{\alpha}(t, u), u \in \left(\frac{(\phi'_2(t)-ct)-\Delta}{\csc\alpha}, \frac{(\phi'_2(t)-ct)+\Delta}{\csc\alpha}\right) \end{cases} \tag{26}$$

Combining (11), (22) and (26),

$$\begin{aligned} FRSST_f^{\alpha}(t, \omega) &= \int_{\Xi_f^{\alpha}} STFRFT_f^{\alpha}(t, u)\delta\left(\omega - \widetilde{\omega}_f^{\alpha}(t, u)\right)du \\ &= \int_{\Xi_{f_1}^{\alpha}} m_1 STFRFT_{f_1}^{\alpha}(t, u)\delta\left(\omega - \widetilde{\omega}_{f_1}^{\alpha}(t, u)\right)du \\ &\quad + \int_{\Xi_{f_2}^{\alpha}} m_2 STFRFT_{f_2}^{\alpha}(t, u)\delta\left(\omega - \widetilde{\omega}_{f_2}^{\alpha}(t, u)\right)du \\ &= m_1 FRSST_{f_1}^{\alpha}(t, \omega) + m_2 FRSST_{f_2}^{\alpha}(t, \omega) \end{aligned} \tag{27}$$

□

(2) Complex Conjugate: If $f(t) \leftrightarrow FRSST_f^{\alpha}(t,\omega)$, it leads to

$$FRSST_{f^*}^{\alpha}(t,\omega) = \left(FRSST_f^{-\alpha}(t,-\omega)\right)^* \tag{28}$$

Proof. Since the $g(t)$ is a real window and the $\cot(\cdot)$ and $\csc(\cdot)$ are odd functions, we can derive

$$\begin{aligned} STFRFT_{f^*}^{\alpha}(t,u) &= \int_{\mathbb{R}} f^*(\tau)g(\tau-t)e^{j\frac{\tau^2-t^2}{2}\cot\alpha - ju(\tau-t)\csc\alpha}d\tau \\ &= \left(\int_{\mathbb{R}} f(\tau)g(\tau-t)e^{j\frac{\tau^2-t^2}{2}\cot(-\alpha) - ju(\tau-t)\csc(-\alpha)}d\tau\right)^* \\ &= \left(STFRFT_f^{-\alpha}(t,u)\right)^* \end{aligned} \tag{29}$$

Furthermore, according to (10),

$$\widetilde{\omega}_{f^*}^{\alpha}(t,u) = \Re\left\{\frac{\partial_t STFT_{f^*}^{\alpha}(t,u)}{jSTFT_{f^*}^{\alpha}(t,u)}\right\} = \Re\left\{-\left(\frac{\partial_t STFT_f^{-\alpha}(t,u)}{jSTFT_f^{-\alpha}(t,u)}\right)^*\right\} = -\widetilde{\omega}_f^{-\alpha}(t,u) \tag{30}$$

which yields

$$\begin{aligned} FRSST_{f^*}^{\alpha}(t,\omega) &= \int_{\Xi_f^{\alpha}} STFRFT_{f^*}^{\alpha}(t,u)\delta\left(\omega-\widetilde{\omega}_{f^*}^{\alpha}(t,u)\right)du \\ &= \int_{\Xi_f^{\alpha}} \left(STFRFT_f^{-\alpha}(t,u)\right)^*\delta\left(\omega-\left(-\widetilde{\omega}_f^{-\alpha}(t,u)\right)\right)du \\ &= \int_{\Xi_f^{\alpha}} \left(STFRFT_f^{-\alpha}(t,u)\right)^*\delta\left(\omega+\widetilde{\omega}_f^{-\alpha}(t,u)\right)du \\ &= \int_{\Xi_f^{\alpha}} \left(STFRFT_f^{-\alpha}(t,u)\right)^*\delta\left(\widetilde{\omega}_f^{-\alpha}(t,u)-(-\omega)\right)du \\ &= \left(\int_{\Xi_f^{\alpha}} \left(STFRFT_f^{-\alpha}(t,u)\right)\delta\left(\widetilde{\omega}_f^{-\alpha}(t,u)-(-\omega)\right)du\right)^* \\ &= \left(FRSST_f^{-\alpha}(t,-\omega)\right)^* \end{aligned} \tag{31}$$

□

(3) Translation: If $f(t) \leftrightarrow FRSST_f^{\alpha}(t,\omega)$, and t_0 is a real number, then

$$FRSST_{f(t-t_0)}^{\alpha}(t,\omega) = FRSST_f^{\alpha}(t-t_0,\omega) \tag{32}$$

Proof. According to (5), we can obtain

$$\begin{aligned} &STFRFT_{f(t-t_0)}^{\alpha}(t,u) \\ &= \int_{\mathbb{R}} f(\tau-t_0)g(\tau-t)e^{j\frac{\tau^2-t^2}{2}\cot\alpha - ju(\tau-t)\csc\alpha}d\tau \\ &= \int_{\mathbb{R}} f(\xi)g(\xi-(t-t_0))e^{j\frac{(\xi+t_0)^2-t^2}{2}\cot\alpha - ju(\xi-(t-t_0))\csc\alpha}d\tau \\ &= \int_{\mathbb{R}} f(\xi)g(\xi-(t-t_0))e^{j\frac{\xi^2-t^2+2tt_0-t_0^2}{2}\cot\alpha - ju(\xi-(t-t_0))\csc\alpha}e^{jt_0\xi\cot\alpha - jt_0t\cot\alpha + jt_0^2\cot\alpha}d\tau \\ &= \int_{\mathbb{R}} f(\xi)g(\xi-(t-t_0))e^{j\frac{\xi^2-(t-t_0)^2}{2}\cot\alpha - j(u-t_0\cos\alpha)(\xi-(t-t_0))\csc\alpha}d\tau \\ &= STFRFT_f^{\alpha}(t-t_0,u-t_0\cos\alpha) \end{aligned} \tag{33}$$

Combining (10) and (33),

$$\widetilde{\omega}_{f(t-t_0)}^{\alpha}(t,u) = \widetilde{\omega}_f^{\alpha}(t-t_0,u-t_0\cos\alpha) \tag{34}$$

Then,

$$\begin{aligned} FRSST^{\alpha}_{f(t-t_0)}(t,\omega) &= \int_{\Xi^{\alpha}_{f}} STFRFT^{\alpha}_{f(t-t_0)}(t,u)\delta\Big(\omega-\widetilde{\omega}^{\alpha}_{f(t-t_0)}(t,u)\Big)du \\ &= \int_{\Xi^{\alpha}_{f}} STFRFT^{\alpha}_{f}(t-t_0,u-t_0\cos\alpha)\delta\Big(\omega-\widetilde{\omega}^{\alpha}_{f}(t-t_0,u-t_0\cos\alpha)\Big)du \\ &= FRSST^{\alpha}_{f}(t-t_0,\omega) \end{aligned} \quad (35)$$

□

(4) Fractional Time Shift: If $f(t) \leftrightarrow FRSST^{\alpha}_{f}(t,\omega)$, and the fractional time shift of $f(t)$ is

$$T^{\alpha}_{t_0}f(t) = f(t-t_0)e^{-jt_0(t-\frac{t_0}{2})\cot\alpha} \quad (36)$$

whereby the STFRFT is

$$FRSST^{\alpha}_{T^{\alpha}_{t_0}f(t)}(t,\omega) = e^{-jt_0(t-\frac{t_0}{2})\cot\alpha}FRSST^{\alpha}_{f}(t-t_0,\omega+t_0\cot\alpha) \quad (37)$$

Proof. Similar to (33), for (36),

$$STFRFT^{\alpha}_{T^{\alpha}_{t_0}f(t)}(t,u) = e^{-jt_0(t-\frac{t_0}{2})\cot\alpha}STFRFT^{\alpha}_{f}(t-t_0,u) \quad (38)$$

Then, combining (10) and (38),

$$\widetilde{\omega}^{\alpha}_{T^{\alpha}_{t_0}f(t)}(t,u) = \widetilde{\omega}^{\alpha}_{f}(t-t_0,u) - t_0\cot\alpha \quad (39)$$

from which, alongside (11), we can derive

$$\begin{aligned} FRSST^{\alpha}_{T^{\alpha}_{t_0}f(t)}(t,\omega) &= \int_{\Xi^{\alpha}_{f}} STFRFT^{\alpha}_{T^{\alpha}_{t_0}f(t)}(t,u)\delta\Big(\omega-\widetilde{\omega}^{\alpha}_{T^{\alpha}_{t_0}f(t)}(t,u)\Big)du \\ &= \int_{\Xi^{\alpha}_{f}} e^{-jt_0(t-\frac{t_0}{2})\cot\alpha}STFRFT^{\alpha}_{f}(t-t_0,u)\delta\Big(\omega-\Big(\widetilde{\omega}^{\alpha}_{f}(t-t_0,u)-t_0\cot\alpha\Big)\Big)du \\ &= e^{-jt_0(t-\frac{t_0}{2})\cot\alpha}FRSST^{\alpha}_{f}(t-t_0,\omega+t_0\cot\alpha) \end{aligned} \quad (40)$$

□

(5) Modulation: For the $f(t)e^{j\omega_0 t}$ with $\omega_0 \in \mathbb{R}$,

$$FRSST^{\alpha}_{f(t)e^{j\omega_0 t}}(t,\omega) = e^{j\omega_0 t}FRSST^{\alpha}_{f}(t,\omega-\omega_0) \quad (41)$$

Proof. Alongside the variable substitution, the STFRFT (5) derives

$$\begin{aligned} STFRFT^{\alpha}_{f(t)e^{j\omega_0 t}}(t,u) &= \int_{\mathbb{R}} f(\tau)e^{j\omega_0\tau}g(\tau-t)e^{j\frac{\tau^2-t^2}{2}\cot\alpha-ju(\tau-t)\csc\alpha}d\tau \\ &= \int_{\mathbb{R}} f(\tau)g(\tau-t)e^{j\frac{\tau^2-t^2}{2}\cot\alpha-j(u-\omega_0\sin\alpha)u(\tau-t)\csc\alpha+j\omega_0 t}d\tau \\ &= e^{j\omega_0 t}STFRFT^{\alpha}_{f}(t,u-\omega_0\sin\alpha) \end{aligned} \quad (42)$$

which, substituted into (10), will allow to obtain

$$\widetilde{\omega}^{\alpha}_{f(at)}(t,u) = \omega_0 + \widetilde{\omega}^{\alpha}_{f}(t,u-\omega_0\sin\alpha) \quad (43)$$

Then,

$$\begin{aligned}
&FRSST^{\alpha}_{f(t)e^{j\omega_0 t}}(t,\omega) \\
&= \int_{\Xi^{\alpha}_f} STFRFT^{\alpha}_{f(t)e^{j\omega_0 t}}(t,u)\delta\Big(\omega - \widetilde{\omega}^{\alpha}_{f(t)e^{j\omega_0 t}}(t,u)\Big)du \\
&= \int_{\Xi^{\alpha}_f} e^{j\omega_0 t} STFRFT^{\alpha}_f(t,u-\omega_0\sin\alpha)\delta\Big(\omega - \Big(\omega_0 + \widetilde{\omega}^{\alpha}_f(t,u-\omega_0\sin\alpha)\Big)\Big)du \\
&= e^{j\omega_0 t} FRSST^{\alpha}_f(t,\omega-\omega_0)
\end{aligned} \tag{44}$$

□

(6) Frequency Shear: For the $f(t)e^{j\frac{b}{2}t^2}$ with $b \in \mathbb{R}$,

$$FRSST^{\alpha}_{f(t)e^{j\frac{b}{2}t^2}}(t,\omega) = e^{j\frac{b}{2}t^2} FRSST^{\sigma}_f(t,\omega-ct) \tag{45}$$

where $\sigma = \operatorname{arccot}(\cot\alpha + b)$.

Proof. Similarly, for the $f(t)e^{j\frac{b}{2}t^2}$,

$$\begin{aligned}
STFRFT^{\alpha}_{f(t)e^{j\frac{b}{2}t^2}}(t,u) &= \int_{\mathbb{R}} f(\tau)e^{j\frac{b}{2}\tau^2} g(\tau-t)e^{j\frac{\tau^2-t^2}{2}\cot\alpha - ju(\tau-t)\csc\alpha}d\tau \\
&= e^{j\frac{b}{2}t^2}\int_{\mathbb{R}} f(\tau)g(\tau-t)e^{j\frac{\tau^2-t^2}{2}(\cot\alpha+b) - j\frac{\csc\alpha}{\csc\sigma}u(\tau-t)\csc\sigma}d\tau \\
&= e^{j\frac{b}{2}t^2} STFRFT^{\sigma}_f\big(t,\tfrac{\csc\alpha}{\csc\sigma}u\big)
\end{aligned} \tag{46}$$

and

$$\widetilde{\omega}^{\alpha}_{f(t)e^{j\frac{b}{2}t^2}}(t,u) = bt + \widetilde{\omega}^{\sigma}_f\Big(t, \frac{\csc\alpha}{\csc\sigma}u\Big) \tag{47}$$

Then,

$$\begin{aligned}
FRSST^{\alpha}_{f(t)e^{j\frac{b}{2}t^2}}(t,\omega) &= \int_{\Xi^{\alpha}_f} STFRFT^{\alpha}_{f(t)e^{j\frac{b}{2}t^2}}(t,u)\delta\Big(\omega - \widetilde{\omega}^{\alpha}_{f(t)e^{j\frac{b}{2}t^2}}(t,u)\Big)du \\
&= \int_{\Xi^{\alpha}_f} e^{j\frac{b}{2}t^2} STFRFT^{\sigma}_f\big(t,\tfrac{\csc\alpha}{\csc\sigma}u\big) \\
&\cdot\delta\Big(\omega - \Big(ct + \widetilde{\omega}^{\sigma}_f\big(t,\tfrac{\csc\alpha}{\csc\sigma}u\big)\Big)\Big)du \\
&= e^{j\frac{b}{2}t^2} FRSST^{\alpha}_f(t,\omega-ct)
\end{aligned} \tag{48}$$

□

4. Numerical Examples

In this section, two examples are employed to show the performance of this new FRSST. At the same time, we take the STFT, FRFT, FSST, and second-order SST (VSST) as the compared methods. For all examples, the sampling frequency, sampling number of the signal, and k are 1000 Hz, 1000, and 150, respectively. Herein, without the loss of generality, all of the methods are conjured with a Gaussian window function.

4.1. Linear Modulations

To show the good resolution and concentration of the new FRSST, we use three different signals, defined as

$$\begin{aligned}
&f_{11}(t) = e^{2\pi j(200t+\frac{k}{2}t^2)} + e^{2\pi j(155t+\frac{k}{2}t^2)}, f_{12}(t) = e^{2\pi j(200t+\frac{k}{2}t^2)} + e^{2\pi j(175t+\frac{k}{2}t^2)}, \\
&f_{13}(t) = e^{2\pi j(200t+\frac{k}{2}t^2)} + e^{2\pi j(195t+\frac{k}{2}t^2)}
\end{aligned} \tag{49}$$

where the frequency intervals of the different modes are decreasing. The corresponding time–frequency representations (TFRs) are shown in Figures 1–3, respectively.

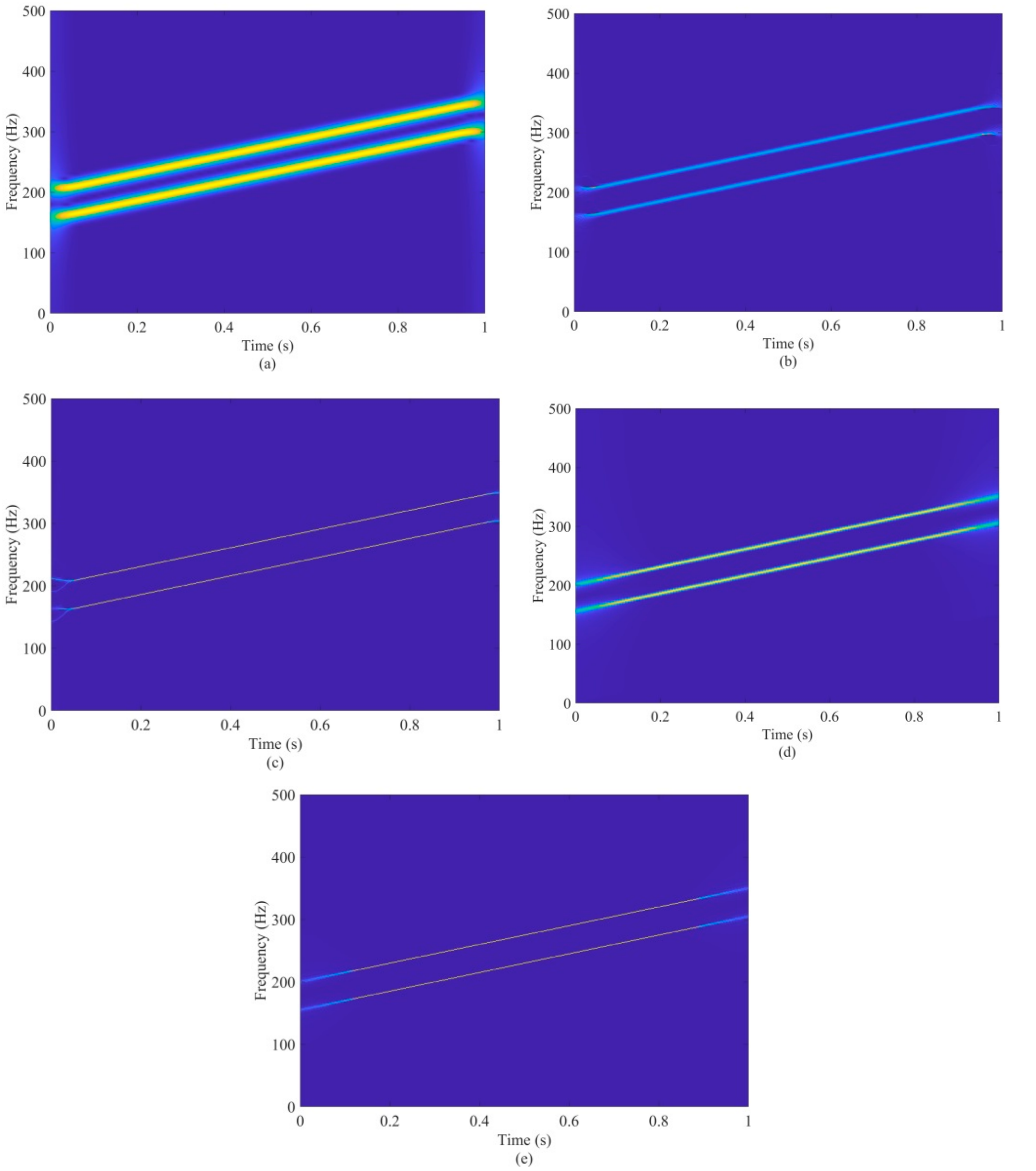

Figure 1. Illustration of the time–frequency representations for signal $f_{11}(t)$ obtained by the (**a**) STFT, (**b**) FSST, (**c**) VSST, (**d**) STFRFT, and (**e**) FRSST.

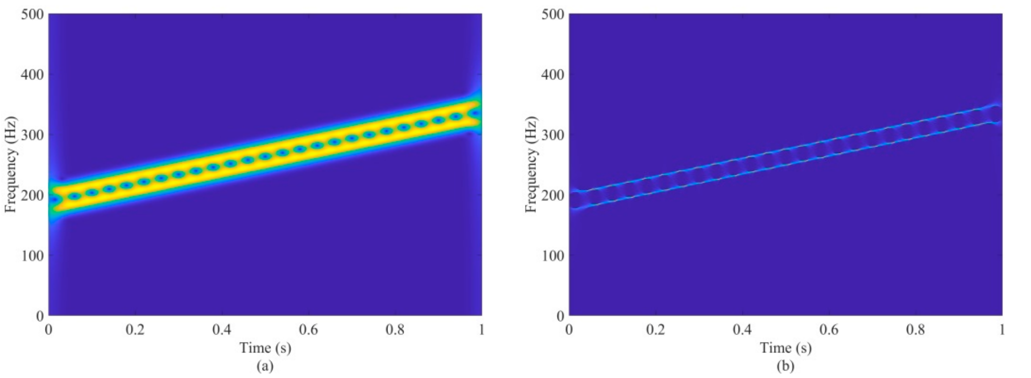

Figure 2. *Cont*.

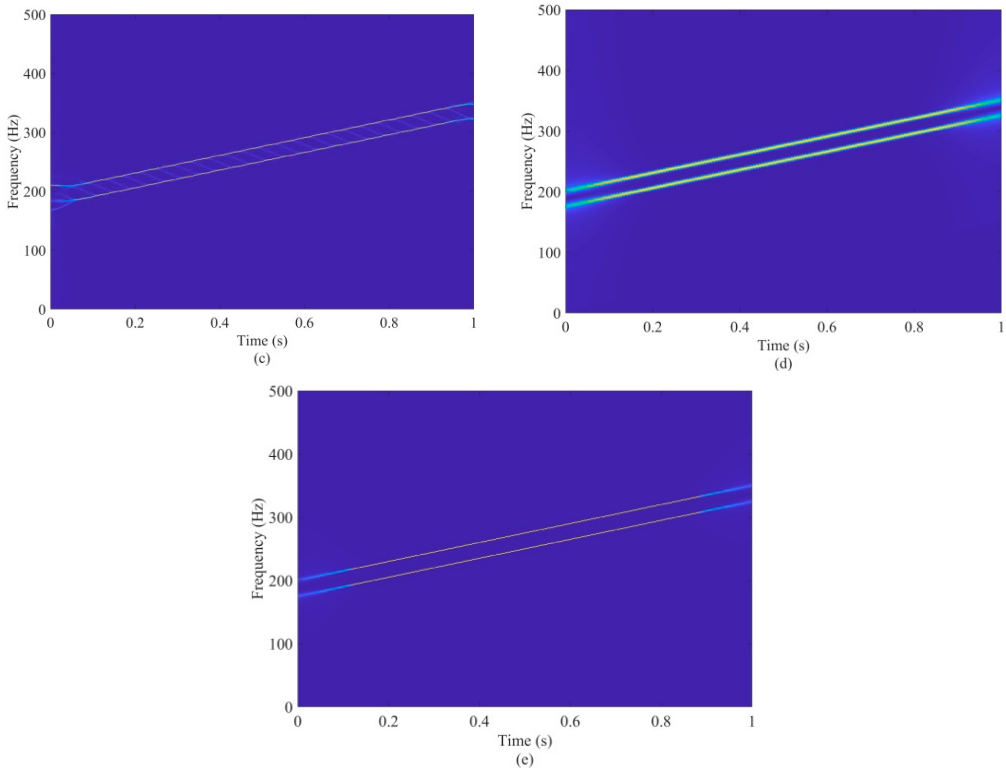

Figure 2. Illustration of the time–frequency representations for signal $f_{12}(t)$ obtained by the (**a**) STFT, (**b**) FSST, (**c**) VSST, (**d**) STFRFT, and (**e**) FRSST.

From Figure 1, it is clear that the five different methods can distinguish the two modes within the signal $f_{11}(t)$. As shown in Figure 1d, the resolution of the STFRFT is still fixed, but it is higher than that of the STFT in Figure 1a. Like the analysis in the other papers [21,22,31], the synchrosqueezing transforms (Figure 1b,c,e) improve the energy concentration of the TFRs. Due to the same underlying assumptions, the FRSST (Figure 1e) can provide a result with the same readability as the VSST (Figure 1c). Moreover, the FRSST inherits the resolution of STFRFT. Thus, compared with the other methods, the proposed FRSST has a better resolution and concentration.

For the signal $f_{12}(t)$, the frequency interval becomes 25 Hz; the TFR is given in Figure 2. We can see that the STFT (Figure 2a) contains cross-terms because of the resolution. Due to the post-processing of the STFT, the FSST (Figure 2b) and the VSST (Figure 2c) improve the concentration of the energy, but still remain less cross-term. The result of the STFRFT is shown in Figure 2d. Due to the improvement in the time–frequency resolution, the STFRFT can still separate the two modes well, but the STFRFT shows low energy concentration. However, the FRSST still exhibits the best performance of resolution and concentration.

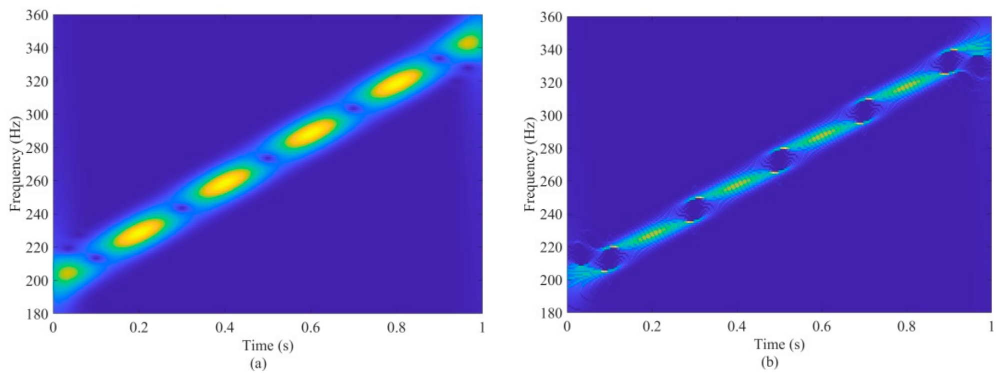

Figure 3. *Cont.*

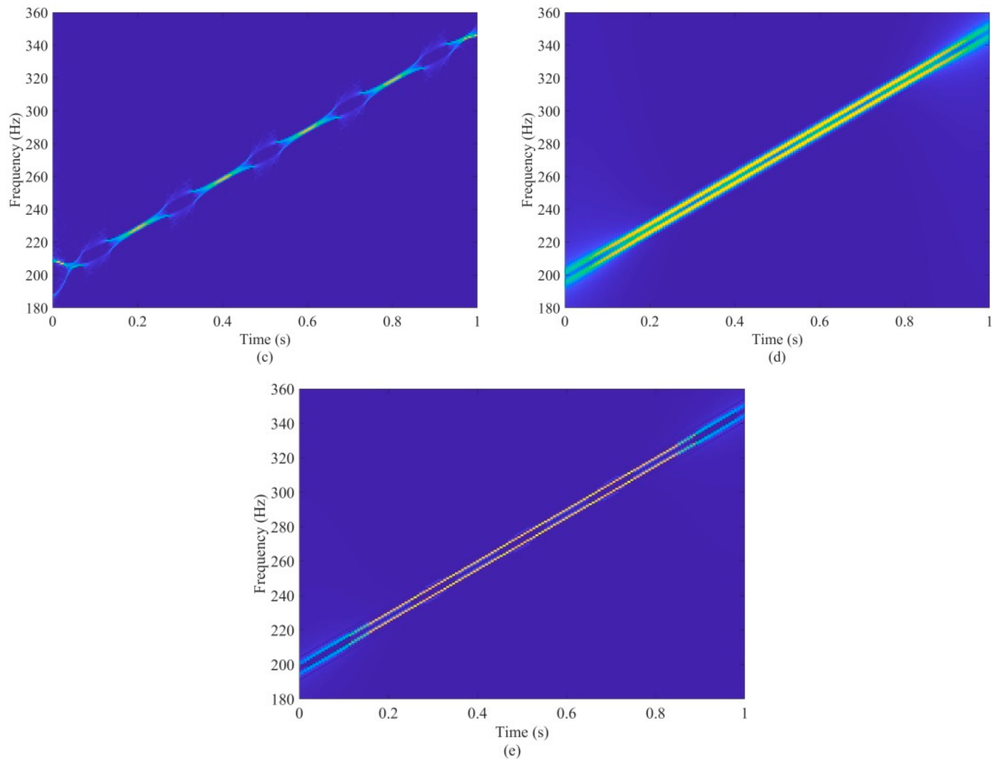

Figure 3. Illustration of the time–frequency representations for signal $f_{13}(t)$ obtained by the (**a**) STFT, (**b**) FSST, (**c**) VSST, (**d**) STFRFT, and (**e**) FRSST.

When the interval reaches 5 Hz in the signal $f_{13}(t)$, the STFT (Figure 3a) cannot identify the features of the two modes in the time–frequency domain, which leads to a useless result. As illustrated in Figure 3b,c, the FSST and VSST share common phenomena of the STFT. As shown in Figure 3d, the two components are well distinguished in the STFRFT domain.

It is worth noting that the FRSST shares the high resolution of the STFRFT and the aggregation of the SST. For the three different frequency intervals of linear frequency-modulated signals, as indicated in Figures 1e, 2e and 3e, the FRSST presents better performance in terms of resolution and concentration, which helps for the subsequent processing and interpretation.

4.2. Linear Modulation with Disturbance

Herein, we take the signal $f_2(t)$ as the second illustration to verify the superiority of the FRSST. The results are shown in Figure 4. The STFT obtains a TFR with diffusion and cross-terms between the two components. It can be seen from Figure 4b that the FSST concentrates the energy of the TFR, but the cross-term still exists and is diffused at the fast-changing frequencies (marked by the white arrow). The STFRFT in Figure 4c provides a TFR that seems to be of the same concentration as that of the STFT. However, the STFRFT can distinguish the two modes clearly and has fewer cross-terms. The conclusions of the theory analysis indicate that the FRSST gives results that can best characterize the TF features of the signal $f_2(t)$.

$$f_2(t) = e^{2\pi j(200t+\frac{k}{2}t^2+cos(3\pi t))} + e^{2\pi j(175t+\frac{k}{2}t^2)} \tag{50}$$

In Definition 1, for the given signal, the window width should be wide enough to ensure that the frequency resolution meets the separation condition. In this case, the time resolution will be poor because of the Heisenberg uncertainty principle. As shown in Figure 5a,b, the low time resolution still leads to the TFR of the STFT and FSST with serious disturbance and energy diffusion. In Figure 5c, the time–frequency resolution of the STFRFT is obviously better than that of the STFT, and the two different modes are separated completely. Unfortunately, the time–frequency distribution is insufficiently concentrated. Like the STFRFT, the FRSST (Figure 5d) can separate the modes. However, the wide window may enlarge the local approximation error, which leads to a bad frequency estimation and then a diffused TFR, indicated by the white arrows in Figure 5d.

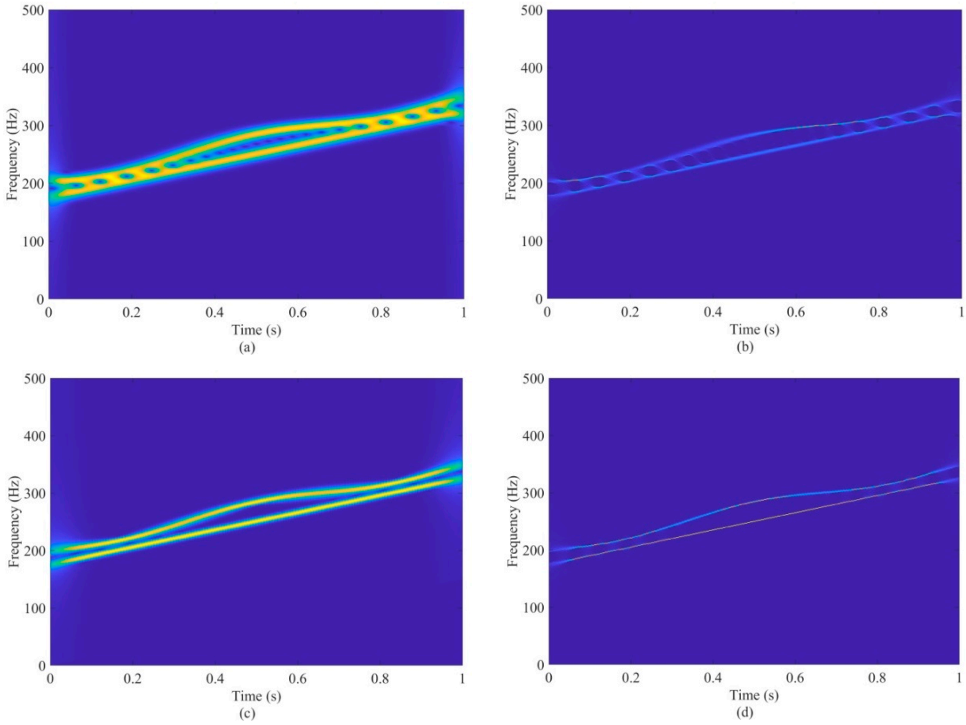

Figure 4. Illustration of the time–frequency representations for signal $f_2(t)$ obtained by the (**a**) STFT, (**b**) FSST, (**c**) STFRFT, and (**d**) FRSST with a suitable window width (number of window samples).

Theorem 1 explains that a narrow window width is required to minimize the error of the frequency estimation. The corresponding results obtained using the four different methods with a narrow window are illustrated in Figure 6. The narrow window width provides a low-frequency resolution, which makes the features of the two modes mixed in the STFT (Figure 6a) or STFRFT (Figure 6c) domain. Though the FSST (Figure 6b) and FRSST (Figure 6d) also have some cross-terms: they are much more concentrated in the TFR because of the good estimation of the instantaneous frequency. In summary, the corresponding results of the FRSST are always more concentrated and can better separate the different components within the signal, i.e., the FRSST provides more flexibility in the choice of window width.

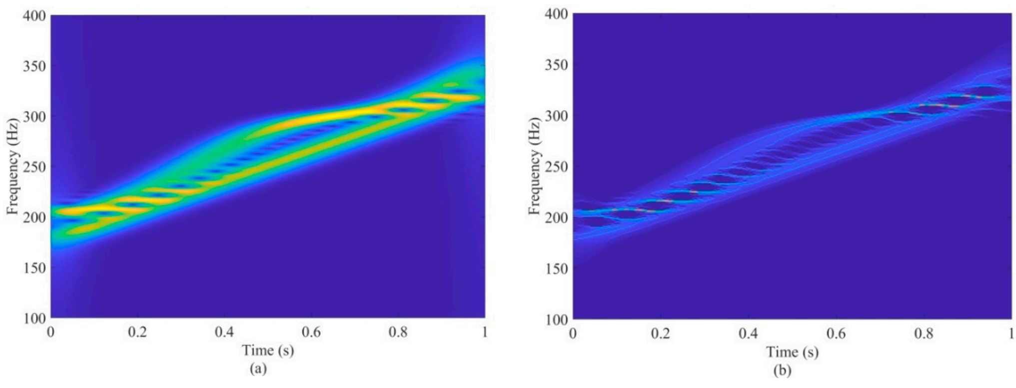

Figure 5. *Cont*.

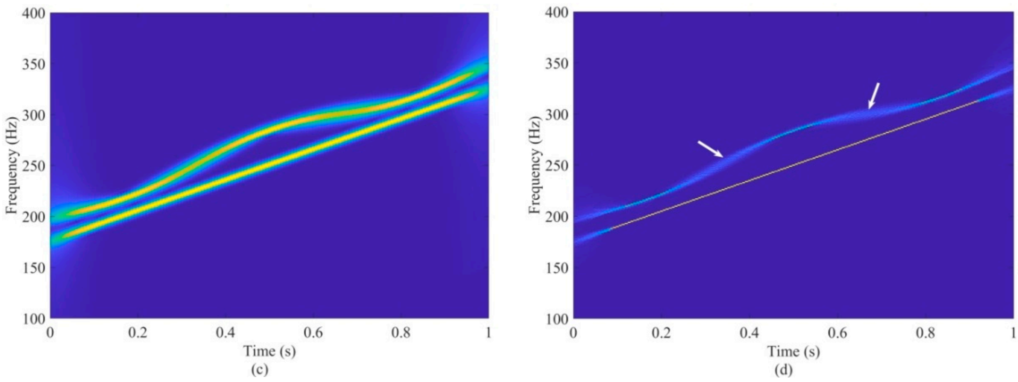

Figure 5. Illustration of the time–frequency representations for signal $f_2(t)$ obtained by the (**a**) STFT, (**b**) FSST, (**c**) STFRFT, and (**d**) FRSST with a wide window width.

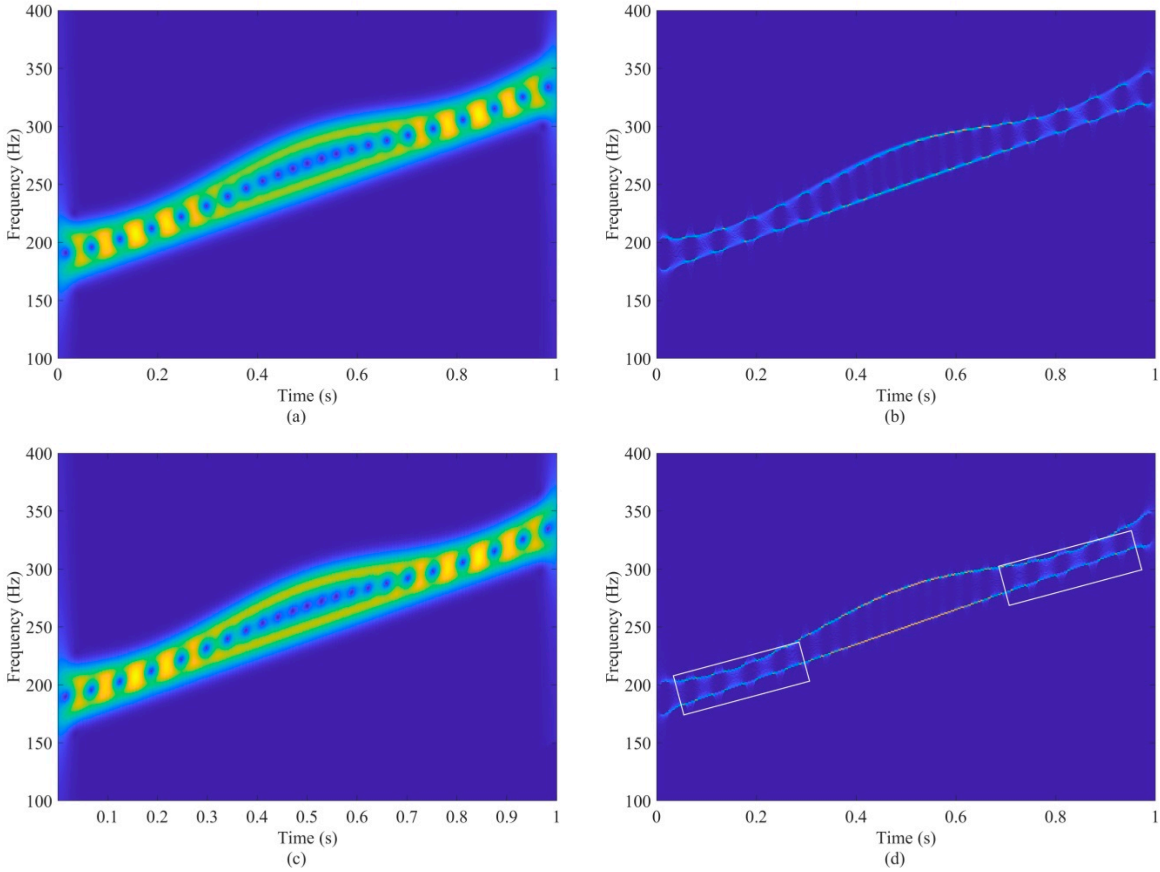

Figure 6. Illustration of the time–frequency representations for signal $f_2(t)$ obtained by the (**a**) STFT, (**b**) FSST, (**c**) STFRFT, and (**d**) FRSST with a narrow window width.

5. Discussion

In the theoretical analysis of the proposed FRSST method, for the signal $f(t) = A(t)e^{j\phi(t)}$, it assumed that $|A'(t)| \leq \varepsilon, |\phi''(t) - c| \leq \varepsilon, \forall t \in \mathbb{R}$. The choice of the angle α is an important point in the implementation of the FRSST. Herein, we consider a linear frequency modulation signal $h(t) = A(t)e^{j\phi(t)} = e^{a_1 + b_1 t + \frac{c_1}{2}t^2} e^{j(a_2 + b_2 t + \frac{c_2}{2}t^2)}$, and the derivative is

$$h'(t) = (b_1 + c_1 t + j(b_2 + c_2 t))h(t) \tag{51}$$

Then, we rewrite Equation (5) as

$$STFRFT_f^{\alpha,g}(u,t) = \int f(\tau+t)g(\tau)e^{j\frac{\tau^2}{2}\cot\alpha + j\tau(t\cot\alpha - u\csc\alpha)}d\tau \tag{52}$$

According to (51) and (52),

$$\begin{aligned}
\partial_t STFRFT_h^{\alpha,g}(u,t) &= \int (b_1 + c_1(\tau+t) + j(b_2 + c_2(\tau+t)))h(\tau+t)g(\tau)e^{j\frac{\tau^2}{2}\cot\alpha + j\tau(t\cot\alpha - u\csc\alpha)}d\tau \\
&\quad + j\cot\alpha \int h(\tau+t)\tau g(\tau)e^{j\frac{\tau^2}{2}\cot\alpha + j\tau(t\cot\alpha - u\csc\alpha)}d\tau \\
&= (b_1 + c_1 t + j(b_2 + c_2 t))\int h(\tau+t)g(\tau)e^{j\frac{\tau^2}{2}\cot\alpha + j\tau(t\cot\alpha - u\csc\alpha)}d\tau \\
&\quad + (c_1 + j(c_2 + \cot\alpha))\int h(\tau+t)\tau g(\tau)e^{j\frac{\tau^2}{2}\cot\alpha + j\tau(t\cot\alpha - u\csc\alpha)}d\tau \\
&= (b_1 + c_1 t + j(b_2 + c_2 t))STFRFT_h^{\alpha,g}(u,t) + (c_1 + j(c_2 + \cot\alpha))STFRFT_h^{\alpha,\tau g}(u,t)
\end{aligned}$$

where $\tau g = \tau g(\tau)$ and $STFRFT_h^{\alpha,\tau g}(u,t)$ are the STFRFT with the window function $\tau g = \tau g(\tau)$. Then,

$$\frac{\partial_t STFRFT_h^{\alpha,g}(u,t)}{STFRFT_h^{\alpha,g}(u,t)} = (b_1 + c_1 t + j(b_2 + c_2 t)) + (c_1 + j(c_2 + \cot\alpha))\frac{STFRFT_h^{\alpha,\tau g}(u,t)}{STFRFT_h^{\alpha,g}(u,t)} \tag{53}$$

Further,

$$b_2 + c_2 t = \Re\left\{\frac{\partial_t STFRFT_h^{\alpha,g}(u,t)}{jSTFRFT_h^{\alpha,g}(u,t)}\right\} - \Re\left\{(-jc_1 + (c_2 + \cot\alpha))\frac{STFRFT_h^{\alpha,\tau g}(u,t)}{STFRFT_h^{\alpha,g}(u,t)}\right\} \tag{54}$$

where $\Re\left\{\frac{\partial_t STFRFT_h^{\alpha,g}(u,t)}{jSTFRFT_h^{\alpha,g}(u,t)}\right\}$ is the operator $\widetilde{\omega}(u,t)$, and it clearly shows that, under the assumed condition $c_2 = -\cot\alpha$. It is the exact estimation of the IF for the constant amplitude linear chirp [46,47]. However, for the linear AM-FM signal, the frequency estimation will diverge from reality.

We use two signals defined by (54) to show the corresponding effect on the time–frequency representation.

$$\begin{aligned}
f_3(t) &= e^{2\pi j(200t + \frac{k_1}{2}t^2)} + e^{2\pi j(130t + \frac{k_2}{2}t^2)}, k_1 = 200, k_2 = 100 \\
f_4(t) &= e^{2\pi j(200t + \frac{k}{2}t^2 + 3cos(6\pi t))}
\end{aligned} \tag{55}$$

The signal $f_3(t)$ consists of two modes with different chirp rates, and the TFRs obtained using the STFRFT and FRSST are given in Figure 7. We can see that the α relates to the concentration of the STFRFT result and the frequency estimation of the FRSST method. In some work concerning the STFRFT, the way to best select the α for multi-component signals was studied. However, in this work, we only consider different modes with the same chirp rate. From the expression of signal $f_4(t)$, it obviously does not meet the assumed conditions. As shown in Figure 8, the TFR is so diffused. In the future, we may consider the higher-order terms of the instantaneous amplitude and phase to extend the FRSST and reduce the influence of α for the concentration of the TFR. Furthermore, we created the algorithm for the proposed method to show the resolution and concentration but do not consider the computation time. The efficiency of the program we have written is low, and this will be the focus of future work.

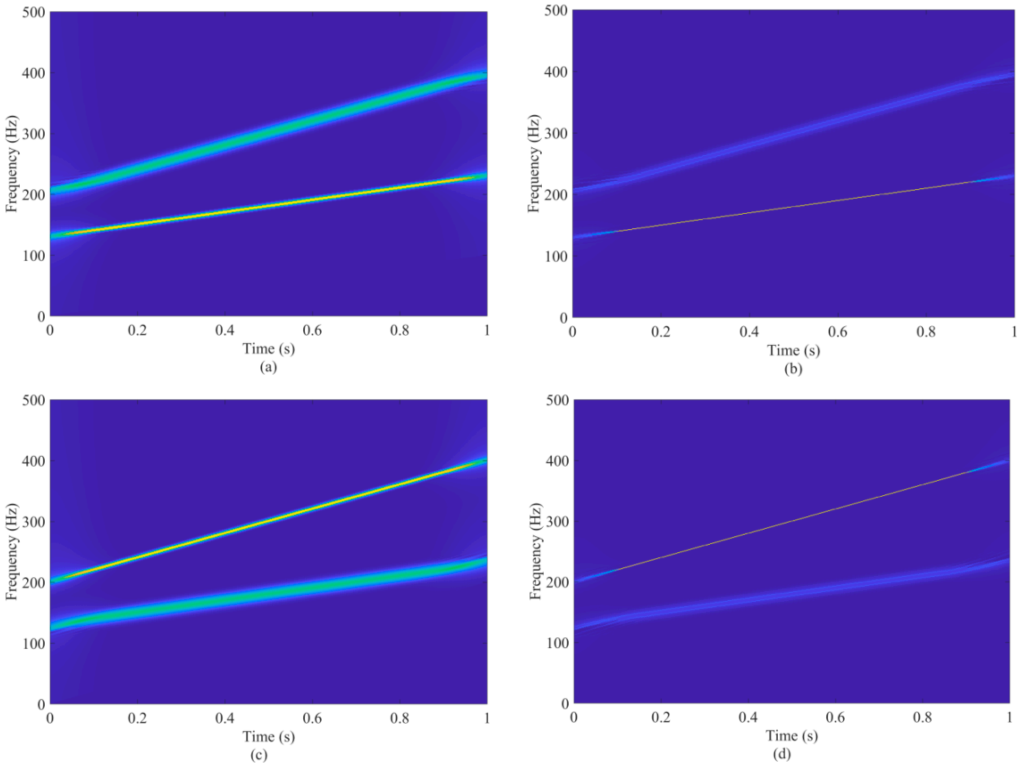

Figure 7. Time–frequency representations of signal $f_3(t)$ from the (**a**) STFRFT, (**b**) FRSST with $\alpha = -\text{arccot}(k_2)$, (**c**) STFRFT, and (**d**) FRSST with $\alpha = -\text{arccot}(k_1)$.

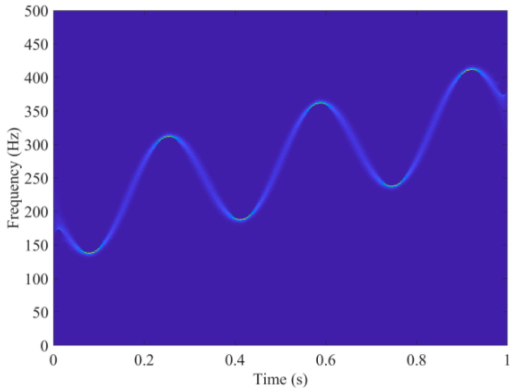

Figure 8. Result of signal $f_4(t)$ obtained using the FRSST.

6. Conclusions

In this paper, we developed a modified novel short-time fractional Fourier transform and then proposed a new extension of the synchrosqueezing short-time Fourier transform (FRSST). Most importantly, we developed a theoretical analysis of the FRSST that states that the energy in the synchrosqueezing time–frequency plane associated with the STFRFT is concentrated around the instantaneous frequency curves $\phi'_n(t)$, and the inverted components $f_n(t)$ approximate the actual oscillatory components $A_n(t)e^{j\phi'_n(t)}$. We also provided the derivation of its basic properties. Numerical examples verified the effectiveness and practicality of the FRSST in terms of the time–frequency resolution and energy concentration, and the results were consistent with the theoretical analysis. Proof of the theoretical limitations is provided in the Section 5, and relevant improvements are currently underway.

Author Contributions: Conceptualization, Z.L. and J.G.; methodology, Z.L. and J.G.; software, Z.G.; validation, Z.G. and L.C.; investigation, Z.L. and L.C.; writing—original draft preparation, Z.L.; writing—review and editing, all authors. All authors have read and agreed to the published version of the manuscript.

Funding: This work was supported by the National Natural Science Foundation of China under Grant 42204116 and 12271428, the National Key Research and Development Program of China under Grant 2020YFA0713403, the Natural Science Basic Research Program of Shaanxi under Grant 2022JQ-230, and by the China Postdoctoral Science Foundation under Grant 2021M692520.

Data Availability Statement: No new data were created or analyzed in this study. Data sharing is not applicable to this article.

Conflicts of Interest: The authors declare no conflicts of interest.

Appendix A

Proof of Proposition 1. Let $\mathrm{B} = \sum_{n=1}^{N} f_n(t)\hat{g}(u\csc\alpha - (\phi'_n(t) - ct))$, which can also be written as

$$\begin{aligned}\mathrm{B} &= \sum_{n=1}^{N} f_n(t)\hat{g}(u\csc\alpha - (\phi'_n(t) - ct)) \\ &= \sum_{n=1}^{N} A_n(t)e^{j\phi_n(t)}\int_{\mathbb{R}} g(\tau - t)e^{-j(\tau-t)(u\csc\alpha - (\phi'_n(t)-ct))}d\tau \\ &= \sum_{n=1}^{N} A_n(t)e^{j\phi_n(t)}\int_{\mathbb{R}} e^{j(\tau-t)(\phi'_n(t)-ct)}g(\tau - t)e^{-j(\tau-t)u\csc\alpha}d\tau\end{aligned} \tag{A1}$$

Then, according to (5), the modified STFRFT of $f(t) \in \mathrm{A}_{\Delta,\varepsilon,c}$ with $\alpha = -\mathrm{arccot}(c)$is

$$\begin{aligned}STFRFT_f^g(t,u) &= \int_{\mathbb{R}} f(\tau)g(\tau-t)e^{j\frac{\tau^2-t^2}{2}\cot\alpha - ju(\tau-t)\csc\alpha}d\tau \\ &= \int_{\mathbb{R}} \sum_{n=1}^{N} A_n(\tau)e^{j\phi_n(\tau)}g(\tau-t)e^{j\frac{\tau^2-t^2}{2}\cot\alpha - ju(\tau-t)\csc\alpha}d\tau \\ &= \sum_{n=1}^{N} e^{j\frac{c}{2}t^2}\int_{\mathbb{R}} (A_n(\tau) - A_n(t))e^{j(\phi_n(\tau) - \frac{c}{2}\tau^2)}g(\tau-t)e^{-ju(\tau-t)\csc\alpha}d\tau \\ &\quad + \sum_{n=1}^{N} e^{j\frac{c}{2}t^2}\int_{\mathbb{R}} A_n(t)e^{j(\phi_n(\tau) - \frac{c}{2}\tau^2)}g(\tau-t)e^{-ju(\tau-t)\csc\alpha}d\tau\end{aligned} \tag{A2}$$

Following from (17) and (A2) is

$$\begin{aligned}STFRFT_f^g(t,u) &= \sum_{n=1}^{N} e^{j\frac{c}{2}t^2}\int_{\mathbb{R}} (A_n(\tau) - A_n(t))e^{j(\phi_n(\tau) - \frac{c}{2}\tau^2)}g(\tau-t)e^{-ju(\tau-t)\csc\alpha}d\tau \\ &+ \sum_{n=1}^{N} A_n(t)e^{j\phi_n(t)}\int_{\mathbb{R}} e^{j(\tau-t)(\phi'_n(t)-ct)} \times e^{\int_0^{\tau-t}(\phi'_n(t+s) - \phi'_n(t) - cs)ds}g(\tau-t)e^{-ju(\tau-t)\csc\alpha}d\tau\end{aligned} \tag{A3}$$

which will obtain

$$\begin{aligned}\left|STFRFT_f^g(t,u) - \mathrm{B}\right| \leq\ & \sum_{n=1}^{N}\int_{\mathbb{R}} |A_n(\tau) - A_n(t)||g(\tau-t)|d\tau \\ &+ \sum_{n=1}^{N} |A_n(t)|\int_{\mathbb{R}} \left|e^{\int_0^{\tau-t}(\phi'_n(t+s) - \phi'_n(t) - cs)ds} - 1\right||g(\tau-t)|d\tau\end{aligned} \tag{A4}$$

From (16),

$$e^{\int_0^{\tau-t}(\phi'_n(t+s) - \phi'_n(t) - cs)ds} - 1 \simeq \int_0^{\tau-t}\left(\phi'_n(t+s) - \phi'_n(t) - cs\right)ds \tag{A5}$$

Then, combining (15), (16), (A4) and (A5),

$$\begin{aligned}
\left|STFRFT_f^g(t,u)-\mathrm{B}\right| \leq\ & \sum_{n=1}^{N}\int_{\mathbb{R}}|A_n(\tau)-A_n(t)||g(\tau-t)|d\tau \\
&+\sum_{n=1}^{N}|A_n(t)|\int_{\mathbb{R}}\left|\int_0^{\tau-t}(\phi'_n(t+s)-\phi'_n(t)-cs)ds\right||g(\tau-t)|d\tau \\
&\leq \sum_{n=1}^{N}\int_{\mathbb{R}}\varepsilon|\tau-t||g(\tau-t)|d\tau+\sum_{n=1}^{N}|A_n(t)|\int_{\mathbb{R}}\left|\int_0^{\tau-t}\varepsilon s ds\right||g(\tau-t)|d\tau \\
&\leq \sum_{n=1}^{N}\int_{\mathbb{R}}\varepsilon|\tau-t||g(\tau-t)|d\tau+\sum_{n=1}^{N}|A_n(t)|\int_{\mathbb{R}}\tfrac{1}{2}\varepsilon|\tau-t|^2|g(\tau-t)|d\tau \\
&= \varepsilon\left(NI_1+\tfrac{1}{2}I_2\sum_{n=1}^{N}|A_n(t)|\right) \\
&= \varepsilon\Gamma_1(t)
\end{aligned} \tag{A6}$$

□

Appendix B

Proof of Proposition 2. According to (A1),

$$\begin{aligned}
\sum_{n=1}^{N}f_n(t)\phi'_n(t)\hat{g}(u\csc\alpha-(\phi'_n(t)-ct)) =\ & \sum_{n=1}^{N}f_n(t)\phi'_n(t)\int_{\mathbb{R}}g(\tau-t)e^{-j(\tau-t)(u\csc\alpha-(\phi'_n(t)-ct))}d\tau \\
&= -j\sum_{n=1}^{N}f_n(t)\int_{\mathbb{R}}g(\tau-t)d\left(e^{-j(\tau-t)(u\csc\alpha-(\phi'_n(t)-ct))}\right)-(u\csc\alpha+ct) \\
&\times\sum_{n=1}^{N}f_n(t)\int_{\mathbb{R}}g(\tau-t)e^{-j(\tau-t)(u\csc\alpha-(\phi'_n(t)-ct))}d\tau \\
&= j\sum_{n=1}^{N}A_n(t)e^{j\phi_n(t)}\int_{\mathbb{R}}g'(\tau-t)e^{-j(\tau-t)(u\csc\alpha-(\phi'_n(t)-ct))}d\tau \\
&-(u\csc\alpha+ct)\sum_{n=1}^{N}f_n(t)\hat{g}(u\csc\alpha-(\phi'_n(t)-ct))
\end{aligned} \tag{A7}$$

Through (A2) and (A3), we can obtain

$$\begin{aligned}
\partial_t STFRFT_f^g(t,u)\ & = \partial_t\int_{\mathbb{R}}f(\tau)g(\tau-t)e^{j\frac{\tau^2-t^2}{2}\cot\alpha-ju(\tau-t)\csc\alpha}d\tau \\
&= -\int_{\mathbb{R}}A(\tau)e^{j\phi(\tau)}g'(\tau-t)e^{j\frac{\tau^2-t^2}{2}\cot\alpha-ju(\tau-t)\csc\alpha}d\tau \\
&+j(u\csc\alpha+ct)\int_{\mathbb{R}}f(\tau)g(\tau-t)e^{j\frac{\tau^2-t^2}{2}\cot\alpha-ju(\tau-t)\csc\alpha}d\tau \\
&= -\sum_{n=1}^{N}e^{j\frac{c}{2}t^2}\int_{\mathbb{R}}(A_n(\tau)-A_n(t))e^{j(\phi_n(\tau)-\frac{c}{2}\tau^2)}g'(\tau-t)e^{-ju(\tau-t)\csc\alpha}d\tau \\
&-\sum_{n=1}^{N}A_n(t)e^{j\phi_n(t)}\int_{\mathbb{R}}e^{\int_0^{\tau-t}(\phi'_n(t+s)-\phi'_n(t)-cs)ds}g'(\tau-t)e^{-j(\tau-t)(u\csc\alpha-(\phi'_n(t)-ct))}d\tau \\
&+j(u\csc\alpha+ct)STFRFT_f^g
\end{aligned} \tag{A8}$$

Combining (A6)–(A8),

$$
\begin{aligned}
&\left|\partial_t STFRFT_f^{\alpha}(t,u) - j\sum_{n=1}^{N} f_n(t)\phi'_n(t)G(u\csc\alpha - (\phi'_n(t)-ct))\right| \\
&= \left|-\sum_{n=1}^{N} e^{j\frac{c}{2}t^2}\int_{\mathbb{R}} (A_n(\tau)-A_n(t))e^{j(\phi_n(\tau)-\frac{c}{2}\tau^2)}g'(\tau-t)e^{-ju(\tau-t)\csc\alpha}d\tau - \sum_{n=1}^{N} A_n(t)e^{j\phi_n(t)}\int_{\mathbb{R}} e^{\int_0^{\tau-t}(\phi'_n(t+s)-\phi'_n(t)-cs)ds}g'(\tau-t)\right. \\
&\quad \times e^{-j(\tau-t)(u\csc\alpha-(\phi'_n(t)-ct))}d\tau + j(u\csc\alpha+ct)STFRFT_f^{g} + \sum_{n=1}^{N} A_n(t)e^{j\phi_n(t)}\int_{\mathbb{R}} g'(\tau-t)e^{-j(\tau-t)(u\csc\alpha-(\phi'_n(t)-ct))}d\tau \\
&\quad \left. -j(u\csc\alpha+ct)\sum_{n=1}^{N} f_n(t)\hat{g}(u\csc\alpha-(\phi'_n(t)-ct))\right| \\
&\le \sum_{n=1}^{N}\int_{\mathbb{R}} |A_n(\tau)-A_n(t)||g'(\tau-t)|d\tau + \sum_{n=1}^{N}|A_n(t)|\int_{\mathbb{R}}\left|\int_0^{\tau-t}(\phi'_n(t+s)-\phi'_n(t)-cs)ds\right||g'(\tau-t)|d\tau \\
&\quad + \left|(u\csc\alpha+ct)\left(STFRFT_f^{g}(t,u)-\mathrm{B}\right)\right| \\
&\le \sum_{n=1}^{N}\int_{\mathbb{R}} \varepsilon|\tau-t||g(\tau-t)|d\tau + \sum_{n=1}^{N}|A_n(t)|\int_{\mathbb{R}}\tfrac{1}{2}\varepsilon|\tau-t|^2|g'(\tau-t)|d\tau + \varepsilon|u\csc\alpha+ct|\Gamma_1(t) \\
&= \varepsilon\left(NI'_1 + \tfrac{1}{2}I'_2\sum_{n=1}^{N}|A_n(t)|\right) + \varepsilon|u\csc\alpha+ct|\Gamma_1(t) \\
&= \varepsilon(\Gamma_2(t) + |u\csc\alpha+ct|\Gamma_1(t))
\end{aligned}
$$

□

Appendix C

Proof of Theorem 1. (a) As the result of Proposition 1,

$$\left|STFRFT_f^{\alpha}(t,u) - \sum_{n=1}^{N} f_n(t)G\big(u\csc\alpha - \big(\phi'_n(t)-ct\big)\big)\right| \le \varepsilon\Gamma_1(t) \tag{A9}$$

Since $supp(G=\hat{g})\subset[-\Delta,\Delta]$, and the frequency interval between every two modes are larger than 2Δ, for any $(t,u)\notin\bigcup_{n=1}^{N} Z_n$, and if

$$\widetilde{\varepsilon} \le \|\Gamma_1\|_{\infty}^{-\frac{1}{2}} \tag{A10}$$

Then

$$\left|STFRFT_f^{\alpha}(t,u)\right| \le \varepsilon\Gamma_1(t) \le \widetilde{\varepsilon}^3\cdot\widetilde{\varepsilon}^{-2} = \widetilde{\varepsilon} \tag{A11}$$

Furthermore, for any $(t,u)\in\mathbb{R}^2$, there is, at most, one n, which satisfies (a). Assuming there exist two integers $n_1 > n_2$ such that $\left|u\csc\alpha - \left(\phi'_{n_1}(t)-ct\right)\right| < \Delta$ and $\left|u\csc\alpha - \left(\phi'_{n_2}(t)-ct\right)\right| < \Delta$. It then holds that

$$
\begin{aligned}
\phi'_{n_1}(t)-\phi'_{n_2}(t) &\le \left|\phi'_{n_1}(t)-\phi'_{n_2}(t)\right| \\
&= \left|u\csc\alpha - \left(\phi'_{n_2}(t)-ct\right) - \left(u\csc\alpha - \left(\phi'_{n_1}(t)-ct\right)\right)\right| \\
&\le \left|u\csc\alpha - \left(\phi'_{n_1}(t)-ct\right)\right| + \left|u\csc\alpha - \left(\phi'_{n_2}(t)-ct\right)\right| \\
&< 2\Delta
\end{aligned} \tag{A12}
$$

which conflicts with $\phi'_{n+1}(t)-\phi'_n(t)\ge 2\Delta$. Thus, for any pair (t,u) under consideration, there is, at most, one mode of the signal $f(t)$ that satisfies $\left|STFRFT_f^{\alpha}(t,u)\right| > \widetilde{\varepsilon}$.

(b) In the Proposition 2, we have the following estimation of $\partial_t STFRFT_f^{g}(t,u)$:

$$\left|\partial_t STFRFT_f^{\alpha}(t,u) - j\sum_{n=1}^{N} f_n(t)\phi'_n(t)G\big(u\csc\alpha - \big(\phi'_n(t)-ct\big)\big)\right| \le \varepsilon(\Gamma_2(t) + |u\csc\alpha+ct|\Gamma_1(t)) \tag{A13}$$

It should be noted that, since the sets Z_n are disjointed, there are no more than two non-zero terms in that involved in the Equations (A9) and (A13). Then, for every $(t,u) \in Z_n$,

$$\begin{aligned}
\left|\widetilde{\omega}_f^{\alpha}(t,u) - \phi'_n(t)\right| = & \left|\frac{\partial_t STFRST_f^g(t,u)}{jSTFRST_f^g(t,u)} - \phi'_n(t)\right| \\
& \leq \left|\frac{\partial_t STFRST_f^g(t,u) - j\sum_{n-1}^{N} f_n(t)\phi'_n(t)G(u\csc\alpha - (\phi'_n(t)-ct))}{jSTFRST_f^g(t,u)}\right| \\
& + \left|\frac{j\phi'_n(t)\left(\sum_{n-1}^{N} f_n(t)G(u\csc\alpha-(\phi'_n(t)-ct)) - STFRST_f^g(t,u)\right)}{STFRST_f^g(t,u)}\right| \\
& \leq \frac{\varepsilon((\Gamma_2(t)+|u\csc\alpha+ct|\Gamma_1(t)))}{\widetilde{\varepsilon}} + \phi'_n(t)\frac{\varepsilon\Gamma_1(t)}{\widetilde{\varepsilon}} \\
& = \widetilde{\varepsilon}^2((\Gamma_2(t) + (|u\csc\alpha + ct| + \phi'_n(t))\Gamma_1(t))) \\
& \leq \widetilde{\varepsilon}^2((\Gamma_2(t) + (2\phi'_n(t) + \Delta)\Gamma_1(t)))
\end{aligned} \tag{A14}$$

Hence, for all t, if it satisfies

$$\widetilde{\varepsilon} \leq \left(\Gamma_2(t) + \left(2\phi'_n(t) + \Delta\right)\Gamma_1(t)\right)^{-1} \tag{A15}$$

Then,

$$\left|\widetilde{\omega}_f^{\alpha}(t,u) - \phi'_n(t)\right| \leq \widetilde{\varepsilon}^2\left(\left(\Gamma_2(t) + \left(2\phi'_n(t) + \Delta\right)\Gamma_1(t)\right)\right) \leq \widetilde{\varepsilon} \tag{A16}$$

(c) According to Reference [33],

$$\begin{aligned}
\lim_{\lambda\to 0}\int_{|\omega-\phi'_n(t)|\leq\widetilde{\varepsilon}} FRSST_f^{\lambda,\widetilde{\varepsilon}}(t,\omega)d\omega \quad & = \frac{\csc\alpha}{2\pi g(0)}\int_{|STFRFT_f^g(t,u)|>\widetilde{\varepsilon}} STFRFT_f^g(t,u) \\
& \times\lim_{\lambda\to 0}\int_{|\widetilde{\omega}_f(t,u)-\phi'_n(t)|\leq\widetilde{\varepsilon}} \frac{1}{\lambda}h\left(\frac{\omega-\widetilde{\omega}_f^{\alpha}(t,u)}{\lambda}\right)d\omega du \\
& = \frac{\csc\alpha}{2\pi g(0)}\int_{|STFRFT_f^g(t,u)|>\widetilde{\varepsilon}\cap|\widetilde{\omega}_f(t,u)-\phi'_n(t)|\leq\widetilde{\varepsilon}} STFRFT_f^g(t,u)du \\
& = \frac{\csc\alpha}{2\pi g(0)}\left[\int_{|STFRFT_f^g(t,u)|>\widetilde{\varepsilon}} STFRFT_f^g(t,u)du\right. \\
& \left. -\int_{|STFRFT_f^g(t,u)|>\widetilde{\varepsilon}\setminus|\widetilde{\omega}_f(t,u)-\phi'_n(t)|\leq\widetilde{\varepsilon}} STFRFT_f^g(t,u)du\right]
\end{aligned} \tag{A17}$$

Alongside (a), for (21),

$$\begin{aligned}
& \left|\lim_{\lambda\to 0}\int_{|\omega-\phi'_n(t)|\leq\widetilde{\varepsilon}} FRSST_f^{\lambda,\widetilde{\varepsilon}}(t,\omega)d\omega - A_n(t)e^{j\phi'_n(t)}\right| \\
= & \left|\frac{\csc\alpha}{2\pi g(0)}\int_{|STFRFT_f^g(t,u)|>\widetilde{\varepsilon}} STFRFT_f^g(t,u)du - A_n(t)e^{j\phi'_n(t)}\right| \\
+ & \left|\frac{\csc\alpha}{2\pi g(0)}\int_{|STFRFT_f^g(t,u)|>\widetilde{\varepsilon}\setminus|\widetilde{\omega}_f(t,u)-\phi'_n(t)|\leq\widetilde{\varepsilon}} STFRFT_f^g(t,u)du\right| \\
\leq & \left|\frac{\csc\alpha}{2\pi g(0)}\int_{|u\csc\alpha-(\phi'_n(t)-ct)|<\Delta}\left[STFRFT_f^g(t,u) - \mathrm{B}\right]du\right| \\
+ & \left|\frac{\csc\alpha}{2\pi g(0)}\int_{|u\csc\alpha-(\phi'_n(t)-ct)|<\Delta} STFRFT_f^g(t,u)du\right| \\
+ & \left|\int_{|u\csc\alpha-(\phi'_n(t)-ct)|<\Delta}\frac{\csc\alpha}{2\pi g(0)}\mathrm{B}du - A_n(t)e^{j\phi'_n(t)}\right| \\
= & \left|\frac{\csc\alpha}{2\pi g(0)}\int_{|u\csc\alpha-(\phi'_n(t)-ct)|<\Delta}(\varepsilon\Gamma_1(t) + \widetilde{\varepsilon})du\right| \\
+ & \left|\frac{\csc\alpha}{2\pi g(0)}\int_{|u\csc\alpha-(\phi'_n(t)-ct)|<\Delta}\mathrm{B}du - A_n(t)e^{j\phi'_n(t)}\right| \\
\leq & \frac{\Delta}{\pi g(0)}(\varepsilon\Gamma_1(t) + \widetilde{\varepsilon}) + 0 \\
= & \frac{2\Delta}{\pi g(0)}\widetilde{\varepsilon}
\end{aligned} \tag{A18}$$

Further, let $C = \frac{2\Delta}{\pi g(0)}$; then, it will be proven that

$$\left| \lim_{\lambda \to 0} \int_{|\omega - \phi'_n(t)| \leq \widetilde{\varepsilon}} FRSST_f^{\lambda,\widetilde{\varepsilon}}(t,\omega)d\omega - A_n(t)e^{j\phi'_n(t)} \right| \leq C\widetilde{\varepsilon}$$

□

References

1. Bracewell, R. *The Fourier Transform and Its Applications*; McGraw-Hill: New York, NY, USA, 1965.
2. Cooley, J.W.; Lewis, P.A.W.; Welch, P.D. The fast Fourier transform and its applications. *IEEE Trans. Educ.* **1969**, *12*, 27–34. [CrossRef]
3. Namias, V. The fractional order Fourier transform and its application to quantum mechanics. *J. Inst. Math. Appl.* **1980**, *25*, 241–265. [CrossRef]
4. Almeida, L.B. The fractional Fourier transform and time-frequency representations. *IEEE Trans. Signal Process.* **1994**, *42*, 3084–3091. [CrossRef]
5. Cohen, L. *Time Frequency Analysis*; Prentice Hall: Englewood Cliffs, NJ, USA, 1995.
6. Gabor, D. Theory of communication. *J. Inst. Electr. Eng.* **1946**, *93*, 429–457. [CrossRef]
7. Morlet, J.; Arens, G.; Fourgeau, E.; Glard, D. Wave propagation and sampling theory-Part I: Complex signal and scattering in multilayered media. *Geophysics* **1982**, *47*, 203–221. [CrossRef]
8. Morlet, J.; Arens, G.; Fourgeau, E.; Glard, D. Wave propagation and sampling theory-Part II: Sampling theory and complex waves. *Geophysics* **1982**, *47*, 222–236. [CrossRef]
9. Grossmann, A.; Morlet, J. Decomposition of Hardy functions into square integrable wavelets of constant shape. *SIAM J. Math. Anal.* **1984**, *15*, 723–736. [CrossRef]
10. Stockwell, R.G.; Mansinha, L.; Lowe, R. Localization of the complex spectrum: The S transform. *IEEE Trans. Signal Process.* **1996**, *44*, 998–1001. [CrossRef]
11. Gao, J.; Chen, W.; Li, Y.; Tian, F. Generalized S transform and seismic response analysis of thin interbeds. *Chin. J. Geophys.* **2003**, *46*, 526–532.
12. Wignaer, E. On the quantum correction for thermodynamic equilibrium. *Phys. Rev.* **1932**, *40*, 749–759. [CrossRef]
13. Ville, J. Theorie et applications de la notion de signal analytique. *Cables Trans.* **1948**, *2A*, 61–74.
14. Mendlovic, D.; Zalevsky, Z.; Lohmann, A.W.; Dorsch, R.G. Signal spatial-filtering using localized fractional Fourier transform. *Opt. Commun.* **1996**, *126*, 14–18. [CrossRef]
15. Zalevsky, Z.; Mendlovic, D.; Caulfield, J.H. Localized, partially space invariant filtering. *Appl. Opt.* **1997**, *36*, 1086–1092. [CrossRef] [PubMed]
16. Ozaktas, H.M.; Kutay, M.A.; Zalevsky, Z. Applications of the fractional Fourier transform to matched filtering, detection, and pattern recognition. In *The Fractional Fourier Transform: With Applications Optics and Signal Processing*; Wiley: New York, NY, USA, 2000; pp. 455–460.
17. Mendlovic, D.; Zalevsky, Z.; Mas, D.; García, J.; Ferreira, C. Fractional wavelet transform. *Appl. Opt.* **1997**, *36*, 4801–4806. [CrossRef] [PubMed]
18. Shi, J.; Liu, X.; Zhang, N. Multiresolution analysis and orthogonal wavelets associated with fractional wavelet transform. *Signal Image Video Process.* **2015**, *9*, 211–220. [CrossRef]
19. Ranjan, R.; Jindal, N.; Singh, A.K. Fractional S-Transform and Its Properties: A Comprehensive Survey. *Wirel. Pers. Commun.* **2020**, *113*, 2519–2541. [CrossRef]
20. Daubechies, I.; Maes, S. A nonlinear squeezing of the continuous wavelet transform based on auditory nerve models. In *Wavelets in Medicine and Biology*; CRC Press: Boca Raton, FL, USA, 1996; pp. 527–546.
21. Daubechies, I.; Lu, J.; Wu, H.T. Synchrosqueezed wavelet transform: An empirical mode decomposition-like tool. *Appl. Comput. Harmon. Anal.* **2011**, *30*, 243–261. [CrossRef]
22. Auger, F.; Flandrin, P. Improving the readability of time-frequency and time-scale representations by the reassignment method. *IEEE Trans. Signal Process.* **1995**, *43*, 1068–1089. [CrossRef]
23. Thakur, G.; Wu, H.T. Synchrosqueezing-based Recovery of Instantaneous Frequency from Nonuniform Samples. *SIAM J. Math. Anal.* **2012**, *43*, 2078–2095. [CrossRef]
24. Oberlin, T.; Meignen, S.; Perrier, V. The Fourier-based synchrosqueezing transform. In Proceedings of the IEEE International Conference on Acoustics, Florence, Italy, 4–9 May 2014; pp. 315–319.
25. Huang, Z.; Zhang, J.; Zou, Z. Synchrosqueezing S-transform and its application in seismic spectral decomposition. *IEEE Trans. Geosci. Remote Sens.* **2016**, *54*, 817–825. [CrossRef]
26. Wang, Q.; Gao, J.; Liu, N.; Jiang, X. High-Resolution Seismic Time-Frequency Analysis Using the Synchrosqueezing Generalized S-Transform. *IEEE Geosci. Remote Sens. Lett.* **2018**, *15*, 374–378. [CrossRef]
27. He, D.; Cao, H.; Wang, S.; Chen, X. Time-reassigned synchrosqueezing transform: The algorithm and its applications in mechanical signal processing. *Mech. Syst. Signal Process.* **2019**, *117*, 255–279. [CrossRef]

28. Yu, G. A Concentrated Time-Frequency Analysis Tool for Bearing Fault Diagnosis. *IEEE Trans. Instrum. Meas.* **2020**, *69*, 371–381. [CrossRef]
29. Li, Z.; Gao, J.; Wang, Z. A Time-Synchroextracting Transform for the Time-Frequency Analysis of Seismic Data. *IEEE Geosci. Remote Sens. Lett.* **2020**, *17*, 864–868. [CrossRef]
30. Li, Z.; Gao, J.; Wang, Z.; Liu, N.; Yang, Y. Time-Synchroextracting General Chirplet Transform for Seismic Time-Frequency Analysis. *IEEE Trans. Geosci. Remote Sens.* **2020**, *58*, 8626–8636. [CrossRef]
31. Oberlin, T.; Meignen, S.; Perrier, V. Second-order synchrosqueezing transform or invertible reassignment? Towards ideal time-frequency representations. *IEEE Trans. Signal Process.* **2015**, *63*, 1335–1344. [CrossRef]
32. Oberlin, T.; Meignen, S. The second-order wavelet synchrosqueezing transform. In Proceedings of the IEEE ICASSP, New Orleans, LA, USA, 5–9 May 2017.
33. Behera, R.; Meignen, S.; Oberlin, T. Theoretical analysis of the second-order synchrosqueezing transform. *Appl. Comput. Harmon. Anal.* **2016**, *34*, 1009. [CrossRef]
34. Han, B.; Zhou, Y.; Yu, G. Second-order synchroextracting wavelet transform for nonstationary signal analysis of rotating machinery. *Signal Process.* **2021**, *186*, 108123. [CrossRef]
35. Yu, G.; Lin, T. Second-order transient-extracting transform for the analysis of impulsive-like signals. *Mech. Syst. Signal Process.* **2021**, *147*, 107069. [CrossRef]
36. Pham, D.; Meignen, S. High-order synchrosqueezing transform for multicomponent signals analysis—With an application to gravitational-wave signal. *IEEE Trans. Signal Process.* **2017**, *65*, 3168–3178. [CrossRef]
37. Lv, S.; Lv, Y.; Yuan, R.; Li, H. High-order synchroextracting transform for characterizing signals with strong AM-FM features and its application in mechanical fault diagnosis. *Mech. Syst. Signal Process.* **2022**, *172*, 108959. [CrossRef]
38. Yu, G.; Yu, M.; Xu, C. Synchroextracting Transform. *IEEE Trans. Ind. Electron.* **2017**, *64*, 8042–8054. [CrossRef]
39. Yu, G.; Wang, Z.; Zhao, P. Multisynchrosqueezing Transform. *IEEE Trans. Ind. Electron.* **2019**, *66*, 5441–5455. [CrossRef]
40. Dong, H.; Yu, G.; Lin, T.; Li, Y. An energy-concentrated wavelet transform for time-frequency analysis of transient signal. *Signal Process.* **2023**, *206*, 108934. [CrossRef]
41. Li, Z.; Gao, J.; Li, H.; Zhang, Z.; Liu, N.; Zhu, X. Synchroextracting transform: The theory analysis and comparisons with the synchrosqueezing transform. *Signal Process.* **2020**, *166*, 107243. [CrossRef]
42. Zhu, X.; Zhang, Z.; Li, Z.; Gao, J.; Huang, X.; Wen, G. Multiple squeezes from adaptive chirplet transform. *Signal Process.* **2019**, *163*, 26–40. [CrossRef]
43. Yu, G.; Lin, R.; Wang, Z.; Li, Y. Time-Reassigned Multisynchrosqueezing Transform for Bearing Fault Diagnosis of Rotating Machinery. *IEEE Trans. Ind. Electron.* **2021**, *68*, 1486–1496. [CrossRef]
44. Chen, X.; Chen, H.; Hu, Y.; Li, R. A statistical instantaneous frequency estimator for high-concentration time-frequency representation. *Signal Process.* **2023**, *204*, 108825. [CrossRef]
45. Zeyani, A.R. Instantaneous Frequency Estimation and Signal Separation Using Fractional Continuous Wavelet Transform. Ph.D. Dissertation, Univ. Missouri St. Louis, St. Louis, MO, USA, 2021.
46. Shi, J.; Chen, G.; Zhao, Y.; Tao, R. Synchrosqueezed Fractional Wavelet Transform: A New High-Resolution Time-Frequency Representation. *IEEE Trans. Signal Process.* **2023**, *71*, 264–278. [CrossRef]
47. Zhao, Z.; Li, G. Synchrosqueezing-Based Short-Time Fractional Fourier Transform. *IEEE Trans. Signal Process.* **2023**, *71*, 279–294. [CrossRef]
48. Shi, J.; Zheng, J.; Liu, X.; Xiang, W.; Zhang, Q. Novel Short-Time Fractional Fourier Transform: Theory, Implementation, and Applications. *IEEE Trans. Signal Process.* **2020**, *68*, 3280–3295. [CrossRef]
49. Zhang, F.; Bi, G.; Chen, Y.Q. Chip signal analysis by using adaptive short-time fractional Fourier transform. In Proceedings of the 10th European Signal Processing Conference, Tampere, Finland, 4–8 September 2000; pp. 1–4.
50. Stankovi'c, L.; Alieva, T.; Bastiaans, M.J. Time-frequency signal analysis based on the windowed fractional Fourier transform. *Signal Process.* **2003**, *83*, 2459–2468. [CrossRef]
51. Tao, R.; Lei, Y.; Wang, Y. Short-time fractional Fourier transform and its applications. *IEEE Trans. Signal Process.* **2010**, *58*, 2568–2580. [CrossRef]